



2D Model to Investigate the Morphological and Hydraulic Changes of Meanders

Jaafar S. Maatooq ^{a*}, Luay K. Hameed ^b

^a Civil Engineering Department, University of Technology, Baghdad, Iraq. 40071@uotechnology.edu.iq

^b Civil Engineering, Department, University of Technology, Baghdad, Iraq. luayk.alwaeli@uokufa.edu.iq

*Corresponding author.

Submitted: 18/03/2019

Accepted: 23/06/2020

Published: 25/1/2020

KEY WORDS

Hydrodynamic,
CCHE2D model,
Meandering,
Experimental model.

ABSTRACT

River engineering investigations require some level of hydrodynamic and morphologic analysis. The detailed of the hydraulic and morphologic features through meander evolution can be recorded by the numerical model spatially and temporally. The Center for Computational Hydro-science and Engineering, two- dimensional model (CCHE2D V3.29) was adopted to investigate the hydraulic and morphologic changes through meander's evolution. Through the experimental work, a series of experiments runs were carried out through combining different geometric and hydraulic parameters to produce different experiment conditions. These parameters are flow rate, bed slope, and different initial incised and wide channels for both rectangular and trapezoidal sections. The CCHE2D model was calibrated and verified using two sets of experimental data. According to the computed values of statistical indicators, BIAS, NSE, and MAE of 0.0084, 0.96, and 0.0132 respectively for water level simulation, and 0.007, 0.94, and 0.0182 respectively for bed level simulation, the calibrated Manning's roughness which gives an acceptable agreement between simulated and measured water and bed levels was 0.029. The verification results were evaluated by the same statistical indicators of BIAS, NSE, and MAE of 0.09, 0.81, and 0.018, respectively, as evidenced by the statistical indicators, values that the CCHE2D model was reasonably capable of simulating the hydraulic and morphological changes through meander evolution.

How to cite this article: J. S. Maatooq and L. K. Hameed, "2D Model to Investigate the Morphological and Hydraulic Changes of Meanders," *Engineering and Technology Journal*, Vol. 38, Part A, No. 1, pp. 9-19, 2020. DOI: <https://doi.org/10.30684/etj.v38i1A.95>

This is an open access article under the CC BY 4.0 license <http://creativecommons.org/licenses/by/4.0>.

1. Introduction

Meandering rivers have a dynamic process, and its platform is changing all the time. These changes significantly affect the hydraulic conditions and morphology. Alluvial meandering channels carry water and deposits resulted from the erosion process in the bed and banks. Many hydraulic factors affect such process, containing: discharge, soil type of banks and bed, channel velocity, section geometry, and vegetation [1]. Such parameters (or some of them) cause numerous changes in the

flow pattern in streamwise and crosswise directions. One of the significant features, which characterize flow in meander bends are secondary currents [2]. The local imbalance between the varying centrifugal force and the transverse-stream pressure gradient results in generating the secondary currents, which combining with the main flow to produce the helical flow [3]. As a result, the sediment is continuously transported by the erosion and deposition action. Erosion usually occurs on the outer banks (concave side) of the channel bends, while deposition takes place on the inner banks (convex side). The formation of riffles, and point bar-pool zones are considered as an essential characteristic of alluvial meandering channels, with pools placed at the apex of meander bends (outer bank), point bar located at (inner bank), and riffles placed at crossings between bends [4,5].

The complete hydraulic and morphologic changes of meander evolution can record by the numerical model spatially and temporally. Therefore, numerous 2D and 3D numerical models have been developed to simulate flow and sediment transport processes in meanders for both laboratory flumes and natural rivers. In practical engineering problems, it is adequate to utilize 2D numerical models to simulate the flow field and sediment transport processes in meanders to reduce the complexity and computational effort (the computation time is reduced). Odgaard [6], Molls and Chaudhry [7] and Hsieh and Yang [8] and others, adopted numerous 2D numerical model to simulate flow and sediment transport in experimental and natural meanders. Zooho et al. cited by Arpan et al. [9] analyzed the variations in the bed of Geum River with the CCHE2D model. Aziaian et al. [10], utilized the CCHE2D model to simulate the unsteady flow and sediment transport in rivers. Taebi et al. [11], presented the numerical simulation of flow using the CCHE2D model in a bend with a 90° angle. He Li et al. [12] analyzed the flow and transport of bed-load in 110° sine-generated meandering flume by the CCHE2D model.

In the present research, the hydrodynamic mobile-bed and banks CCHE2D V3.29 model with non-uniform sediment was adopted to simulate the hydraulic and morphologic changes of experimental alluvial channel through meanders evolution.

2. Materials and Methods

1. Experiments setup and measurement method

The experiments were carried out in a concrete flume having total length= 7 m, depth=0.22 m, and width= 1.5 m. The water is circulated by a centrifugal pump, with discharge levels being determined by the calibrated flow meter. Figure 1 illustrates the schematic of the top and side of the flume, respectively.

The water was circulated by a centrifugal pump, with discharge levels being determined by the calibrated flow meter. The discharge was varied by a controlling valve, which can be controlled manually utilizing a lever. Figure 2 shows the experimental flume and the initial straight channel carved in the center of the flume with initial the bend at the upstream of the flume. The first bend is a short entrance channel used as an initial upstream disturbance to develop patterns of the meander. This initial bend was formed at an angle of (30° – 40°) to the longitudinal axis of the flume; this procedure has been used by most researchers [4,5,13]. So it was extensively proved by pioneer researchers in achieving the meandering processes. The selected sediment used in the experiments runs non-cohesive, non-uniform alluvial sediment.

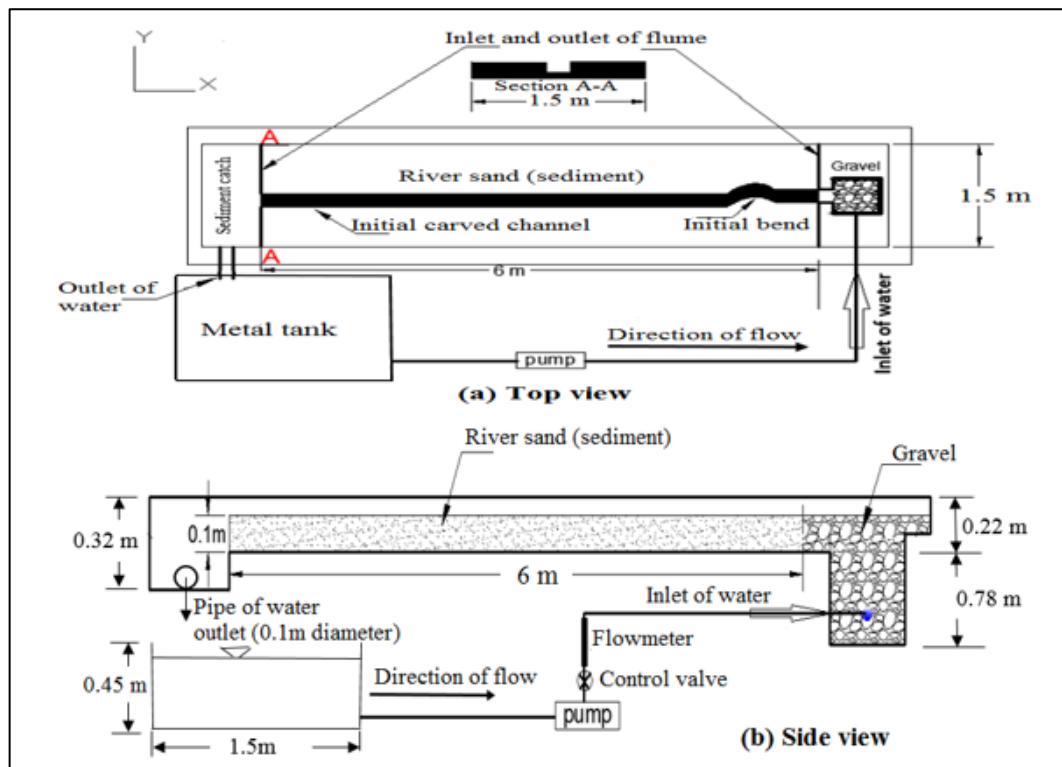


Figure 1: Schematic of the experimental flume (a) top view and (b) side view

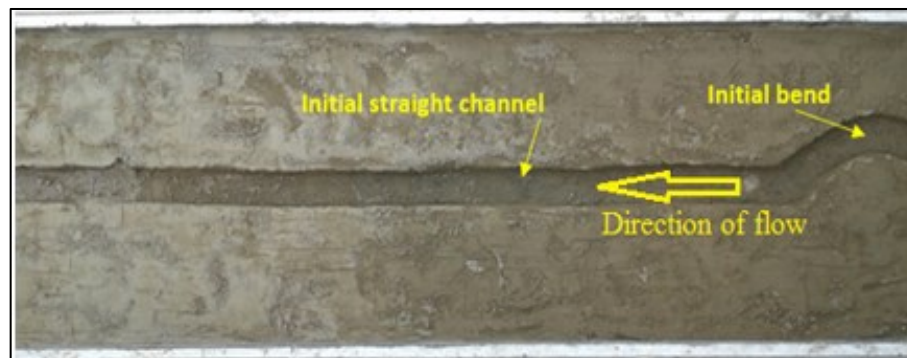


Figure 2: Initial Straight channel with an initial bend prepared for experiment

The median size d_{50} for the selected sand is 0.3mm, and its specific gravity is about 2.68. The degree of uniformity of the particle size distribution was defined by the value of its geometric standard deviation σ_g , which was represented by $\sigma_g = (d_{84}/d_{16})^{0.5}$ and equal to 3.8. Accordingly, the sand used in this study was nonuniform [14]), and classified as poorly graded sand-silty according to USCS (Unified Soil Classification System).

Numerous experiments have been undertaken in this study. Different initial incised and wide channels for both rectangular and trapezoidal sections, two flow rates, two initial bed slopes were combined to make various experimental conditions. Experiment conditions for all cases are presented in Table 1. The experiment conditions presented in Table 1 illustrate, as an example, the adopted range of flow and geometric conditions. The hydraulic conditions subject to the current experiments were selected to satisfy the hydraulic conditions to be consistent with the context of the flow usual in the rivers where the hydraulic conditions have been selected to achieve; subcritical flow (Froude number <1), fully turbulent flow (Reynolds number > 10000), and sediment transport ($\bar{u} > \bar{u}_{cr}$), where \bar{u} =depth average velocity and \bar{u}_{cr} = critical depth-averaged velocity sufficient to move sand along the bed and to erode the banks.

Table 1: Geometric and hydraulic parameters in the experiment runs

Experiment Runs	Initial Channel cross section (cm ²) Width x depth x side slope angle	Area of transverse section (cm ²)	Flow rate (l/sec)	Initial bed slope	width/bank depth ratio	notes
The experiments series A for initial rectangular section						
A-1	14×6	84	1.33	0.005	2.33	Incised rectangular channel
A-2	18×9	162	3	0.005	2	=
A-3	14×6	84	1.33	0.01	2.33	=
A-4	18×9	162	3	0.01	2	=
A-5	24×4	96	1.33	0.005	6	Wide rectangular channel
A-20	20×9	180	5	0.01	2.2	=
The experiments series B for initial trapezoidal section						
B-9	14×6×45°	120	1.33	0.005	4.33	Incised trapezoidal channel
B-10	16×7×45°	161	3	0.005	4.28	=
B-13	18×5×45°	115	1.33	0.005	5.6	Wide trapezoidal channel
B-44	16×9×45°	268	5	0.01	4.8	Incised trapezoidal channel

The first step in the analysis is that the flume was filled with sand to a depth of 10-15, cm and the surface leveled by scraper and carefully graded to the adopted slope. The channel is then carved along the centerline by creating an initial bend at the upstream. The width/bank depth ratio has been adopted to classify the case of the channel i.e., incised or wide. If the width/bank depth ratio is less than 5, the channel is considered as incised. Otherwise, the channel is wide [15,16]. The experimental runs start as the flow was beginning to supply the initial straight channel. The bed and banks start to deform, which lead to the development of meanders. This process continues until the equilibrium state is reached when the number of changes in the channel cross-section, meandering path, and its migration can be neglected, and the longitudinal profile of the water surface is approximately constant.

II. CCHE2D model

CCHE2D model is a package for 2D simulation of open channel flows, sediment transport and morphological processes with mobile bed and banks both in the laboratory and nature. The governing equations of the flow model are differential equations of two-dimensional depth-averaged of the continuity equation;

$$\frac{\partial Z}{\partial t} + \frac{\partial(hu)}{\partial x} + \frac{\partial(hv)}{\partial y} = 0 \quad (1)$$

And momentum equations;

$$\frac{\partial u}{\partial t} + u \frac{\partial u}{\partial x} + v \frac{\partial u}{\partial y} = -g \frac{\partial Z}{\partial x} + \frac{1}{h} \left[\frac{\partial(h\tau_{xx})}{\partial x} + \frac{\partial(h\tau_{xy})}{\partial y} \right] - \frac{\tau_{bx}}{\rho h} + f_{Cor} v \quad (2)$$

$$\frac{\partial v}{\partial t} + u \frac{\partial v}{\partial x} + v \frac{\partial v}{\partial y} = -g \frac{\partial Z}{\partial y} + \frac{1}{h} \left[\frac{\partial(h\tau_{yx})}{\partial x} + \frac{\partial(h\tau_{yy})}{\partial y} \right] - \frac{\tau_{by}}{\rho h} + f_{Cor} u \quad (3)$$

Where u and v are the depth-integrated velocity components in the x and y directions respectively; g is the acceleration due to gravity; h is the local water depth, Z is the water surface elevation; ρ is water mass density; τ_{xx} , τ_{xy} , τ_{yx} , and τ_{yy} are the depth integrated Reynolds stresses; τ_{bx} and τ_{by} are shear stresses on the bed surface along the x and y directions respectively, and f_{Cor} is the

Coriolis force parameter due to earth's rotation. The depth-averaged transport equation of suspended sediment is;

$$\frac{\partial(hC_k)}{\partial t} + \frac{\partial(uhC_k)}{\partial x} + \frac{\partial(vhC_k)}{\partial y} = \frac{\partial}{\partial x} \left(\varepsilon_s h \frac{\partial C_k}{\partial x} \right) + \frac{\partial}{\partial y} \left(\varepsilon_s h \frac{\partial C_k}{\partial y} \right) + \frac{\partial S_x}{\partial x} + \frac{\partial S_y}{\partial y} + \alpha \omega_{sk} (C_{*k} - C_k) \quad (4)$$

In which ($k=1, 2, \dots, N$) represents a sediment size class; and N is the total number of size classes; h is the local water level; u and v are the depth-integrated velocity components in the x and y directions respectively; C_k is the depth-averaged suspended-load concentration of the k -th size class; C_{*k} is the suspended-load transport capacity or the depth-averaged suspended-load concentration at the equilibrium state; ε_s is the turbulence diffusivity coefficient of sediment, determined with $\varepsilon_s = \frac{v_t}{\sigma_c}$, in which σ_c is the turbulent Schmidt number, usually having a value between 0.5 and 1.0, ω_{sk} is the settling velocity of sediment; α is the non-equilibrium adaptation factor having a value of 0.5, and S_y and S_x are the dispersion terms to account for the effect of the nonuniform distributions of flow velocity and sediment concentration [17]. The bed-load transport is determined by;

$$\frac{\partial(\delta_b C_{bk})}{\partial t} + \frac{\partial(\alpha_{bx} q_{bk})}{\partial x} + \frac{\partial(\alpha_{by} q_{bk})}{\partial y} = \frac{1}{L_t} (q_{bk} - q_{b*k}) = 0 \quad (5)$$

Where, C_{bk} is the average concentration of bed load at the bed-load zone; q_{bk} is the bed-load transport rate of size class k ; L_t is the adaptation length for bed load; q_{b*k} is the corresponding bed-load transport capacity or bed-load transport rate at the equilibrium state; and α_{bx} and α_{by} are the direction cosine components of bed load movement, which is assumed to be along the direction of bed shear. In case of meanders, α_{bx} and α_{by} are corrected to consider the effects of helical motions.

Turbulence models are adopted in the CCHE2D numerical model to estimate the eddy viscosity. For the sediment transport simulation. The depth averaged differential equations of sediment transport models for both bed load and suspended load to conduct the spatial and temporal morphological changes in rivers. The numerical solution adopted by CCHE2D model based on a hybrid numerical method, which depend on a mixed finite element, and finite volume method. Software versions utilized for present study were CCHE-MESH V3.0 and CCHE2D V3.29. The mesh generator is used to prepare the mesh for the physical domain. The CCHE2D model is used to assign the flow and sediment parameters, computation parameters, initial and boundary conditions, conduct the numerical simulation, and visualize the simulation results. More description of the CCHE2D model can be found in [17].

III. Method of model calibration and validation

It is necessary to calibrate the numerical model and finding the mean of resistance to the flow to correspond with the experimental measurements. The resistance to the flow is represented by a roughness coefficient which varies with characteristics of sediment, bed form, meander geometry, meander planform and vegetation, etc. Manning's roughness coefficient is widely appropriate for roughness in river modeling (CCHE2DV3.29 Manual). The experimental run B-10 was used for the calibration process. The flowrate of this experiment represents approximately the average value of the undertaken flow rate values as well as the initial geometry is incised, so it will be possible to generate high stream power to erode the channel bank lines and will be able to form the secondary currents, which are the main responsible for bank erosion and meandering formation so, it is expected to achieve total resistance. The boundaries of the experimental flume were defined by importing the experimental initial channel picture with extension (*. bmp) as shown in Figure 3. The cross sections were added to the predefined channel boundaries by adding the data coordinates file which having extension of (*. mesh_xyz) as shown in Figure 4.

As the general academic criteria, the orthogonality and smoothness are usually used to assess the mesh quality quantitatively. Different algebraic meshes were generated with different values of structured lines based on the measured cross-sections of the primary channel. These structured lines are I-lines across the channel (crosswise-direction) and J-lines along the channel (streamwise-direction). An algebraic mesh was generated with 6100 nodes ($I \times J$). Figure 5 shows the CCHE2D model for experimental run B-10. Flow and geometric data for the experiment run B-10 and A-1

were used to calibrate and verify the numerical CCHE2D model. Table 2 illustrates the boundary conditions for the calibration and verification process.

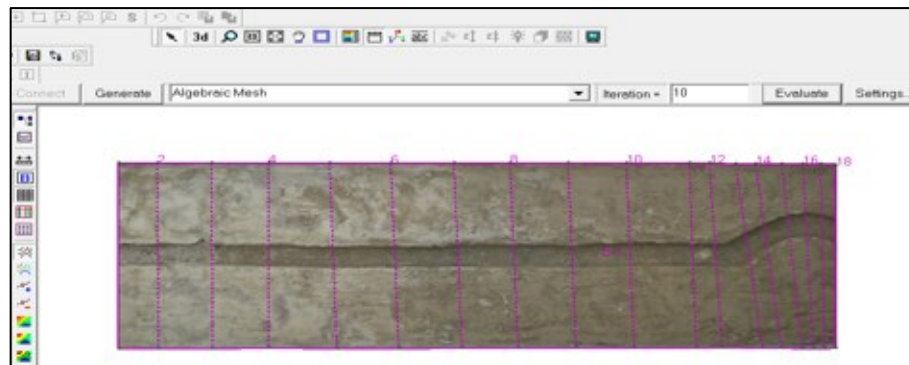


Figure 3: Define the boundaries of the initial channel

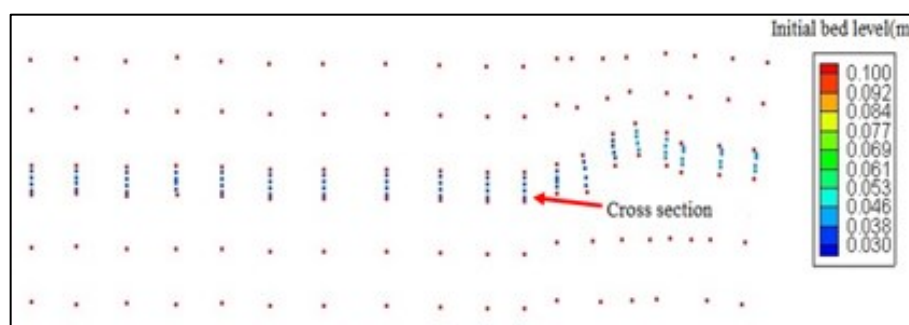


Figure 4: Adding (*. mesh_xyz) data file to the predefined initial channel

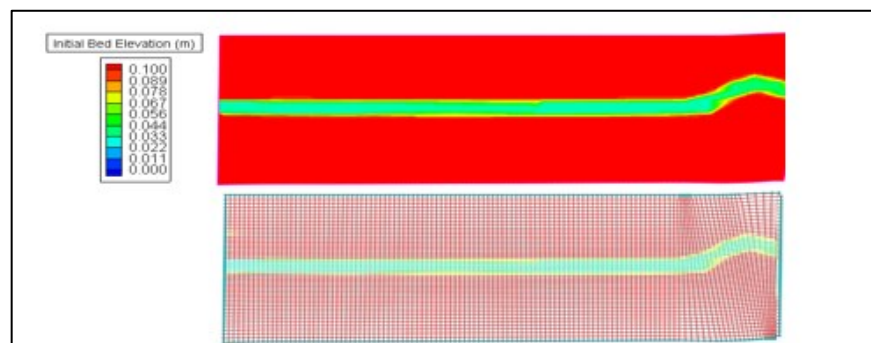


Figure 5: CCHE2D model for experimental run B-10

Table 2: Initial and Boundary Conditions for calibration and verification process

Experimental run	Upstream boundary condition (inlet discharge L/sec)	Downstream boundary condition (outlet water depth)	Duration of simulation (sec)	Remarks
B-10	3	0.05m	35400	Calibration process
A-1	1.33	0.04m	28800	Verification process

The duration of simulation was used as equilibrium state time obtained from the experiment run (to be consistent). Flow simulation must be completed first and then the sediment transport simulation can be performed. To simulate the morphologic changes in nonuniform sediment, the sediment mixture was divided into 7- size classes to define the compositions of bed material for the entire domain. Figure 6 shows the 7- size classes and the fractions of each size class used in the sediment transport simulations.

According to the strikler equation, the value of the manning roughness coefficient due to grain roughness with the horizontal bed, $n=Ck_s^{1/6}$, where $C= 0.034$ for natural sediment and $k_s=d_{50}$ (d_{50} in ft.) [18]. Accordingly, the value of n was calculated and equal to 0.017. This initial roughness value was assigned to each element of the mesh and iteratively adjusted through the calibration process until the model sufficiently simulated the measured data. The calibration results were evaluated by the statistical indicators of the Nash-Sutcliffe efficiency (NSE), Bias, and mean absolute error (MAE).

$$NSE = 1 - \left[\frac{\sum_{i=1}^N (X_{exp} - X_{pred})^2}{\sum_{i=1}^N (X_{exp} - \bar{X}_{exp})^2} \right] \quad (6)$$

$$BIAS = \frac{1}{N} \sum_{i=1}^N (X_{pred} - X_{exp}) \quad (7)$$

$$MAE = \frac{1}{N} \sum_{i=1}^N |X_{pred} - X_{exp}| \quad (8)$$

Where, X_{pred} and X_{exp} are the predicted and measured value, respectively; N is the total measurements. NSE value of 1 corresponds to a perfect match between simulated and observed data. Values of NSE between 0 and 1 are generally indicated as acceptable levels of performance. Bias measures the tendency of the predicted values to be larger or smaller than their observed ones. The optimal value is 0, positive values indicate a tendency to overestimation, and negative values indicate a tendency to underestimation. MAE values of 0 indicate an optimal fit.

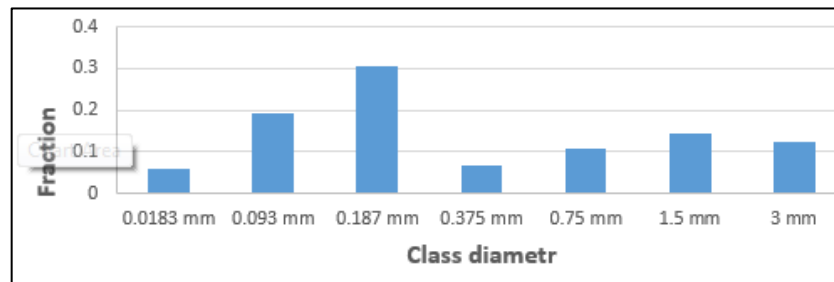


Figure 6: The 7- size classes and the fractions of each size class

3. Results and Discussion

3.1. Model calibration

Calibrations performed with different roughness values starting from the value estimated from the strikler equation. Water level simulations were performed for experimental run B-10 at $t=60$ min using different Manning's n . Table 3 lists the statistical evaluation of calibration results of the water and bed level profiles for experimental run B-10 at $t=60$ min with different values of Manning's roughness. According to the statistical evaluation of BIAS, NSE, and MAE, the calibrated Manning's roughness, which gives an acceptable agreement between simulated and measured water and bed level was 0.029. Accordingly, the calibration process was ended. Through the evolution of meander, it was observed that the bedforms, morphological features (pools and point bars), irregularity in cross-sections, and planform were developed which lead to an increase in the Manning coefficient. Figure 7 and Figure 8 show the measured and simulated water and bed level profiles for an experiment run B-10 at $t=60$ min with n of 0.029.

The simulated morphological features of pools and point bars were reasonably reproduced when compared with the experiment run B-10 at 60 min, as shown in Figure 9. This might be that the current version of CCHE2D incorporates secondary currents effects that occur as a result of the curvature of the channel.

Another simulated morphological feature of the thalweg line and the spatial delineation of bank lines reproduced well when compared with experimental ones, as shown in Figure 10.

Table 3: Model calibration in terms of the experiment run B-10 at t=60min

Exp. run	Case	n	BIAS	NSE	MAE
B-10	Water level profile	0.017	-0.011	0.81	0.019
		0.02	0.019	0.86	0.0181
		0.023	0.012	0.867	0.0169
		0.026	0.009	0.91	0.0131
		0.029	0.0084	0.96	0.0132
		0.03	0.0091	0.93	0.014
	Bed level profile	0.017	0.016	0.86	0.026
		0.02	0.01	0.875	0.021
		0.023	0.0083	0.91	0.0183
		0.026	0.0075	0.94	0.018
		0.029	0.007	0.94	0.0182
		0.03	0.0079	0.93	0.0189

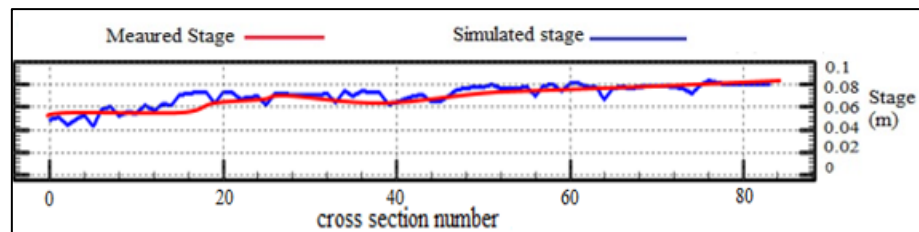


Figure 7: the measured and simulated water level profile for experiment run B-10 at t=60 min with n of 0.029

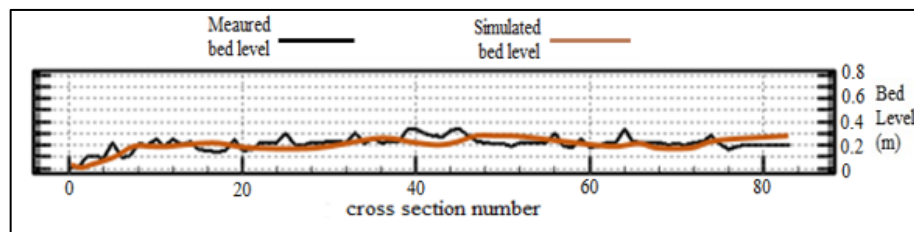


Figure 8: the measured and simulated bed level profile for experiment run B-10 at t=60 min with n of 0.029

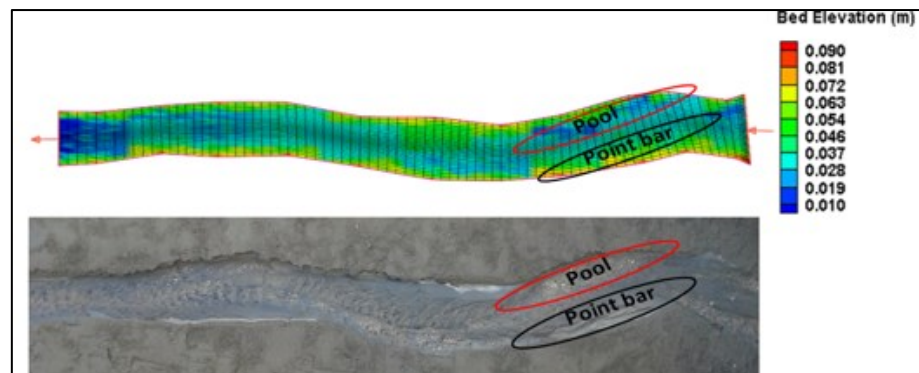


Figure 9: Simulated and observed morphological features for run B-10 at t=60 min, n=0.029

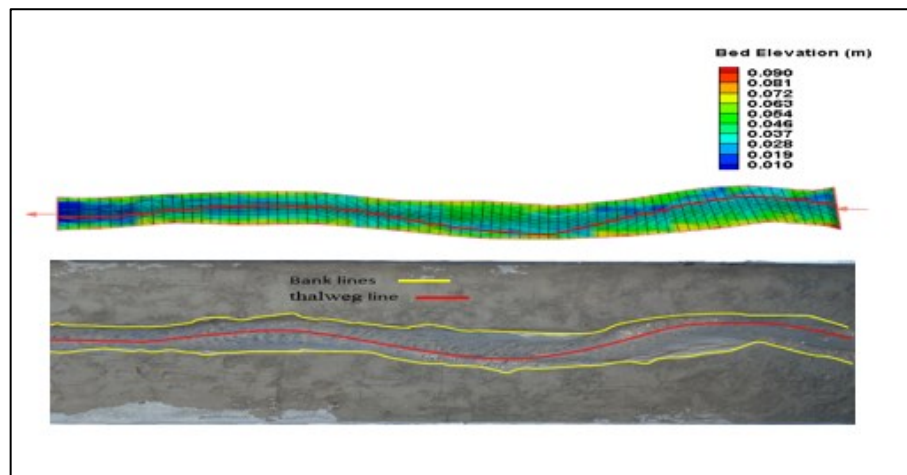


Figure 10: Simulated and observed thalweg and bank lines for exp. run B-10 at $t=60$ min, $n=0.029$

Experimental run B-10 at $t=530$ min was used to compare the simulated and measured cross-sections at specified locations, as shown in Figure 11. For CS2, the simulated bed elevation was slightly over-estimated in the middle of the cross-section, and the two banks were somewhat shifted to the right compared with experimental ones. In addition, For CS1 and CS3, the simulation correctly predicted the pool depth (scour). In contrast, the point bar height (deposition) were somewhat over-estimated, and the right banks for both cross-sections were slightly shifted to the left compared with experimental ones.

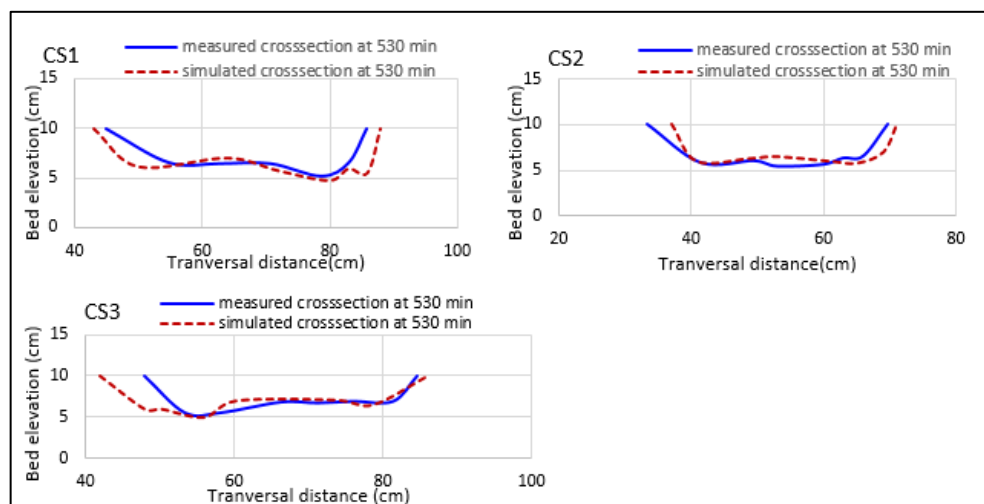


Figure 11: Comparisons between simulated and measured cross sections at 530 min for experiment run B-10 at specified locations

II. Model validation

Experimental run A-1 at $t=300$ min was used to verify the calibrated model on its ability to reproduce the measured profiles using the case of low discharge (i.e., 1.33l/sec). Figure 12 and Figure 13 show the simulated and observed water and bed level profiles, respectively. The verification results were evaluated by the statistical indicators of Bias and mean absolute error (MAE) along with the Nash-Sutcliffe efficiency (NSE). The obtained values of Bias, NSE, and MAE were 0.09, 0.81, and 0.018, respectively, which indicated good agreement between the simulated and measured water level profiles. In addition, the obtained values of Bias, NSE, and MAE were 0.12, 0.73, and 0.012, respectively, which indicated reasonably agreement between the simulated and measured bed level profiles. Therefore, the verification was satisfactory.

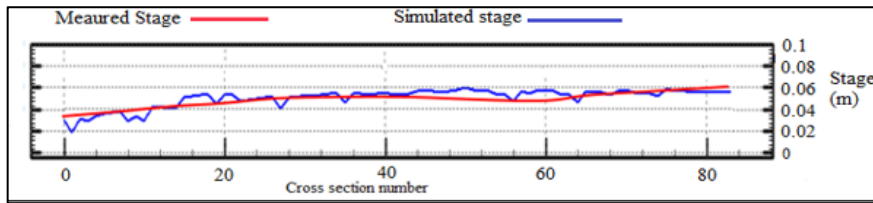


Figure 12: Simulated and observed water surface profile at the centerline for exp. run A-1 at $t=300$ min, $n=0.029$

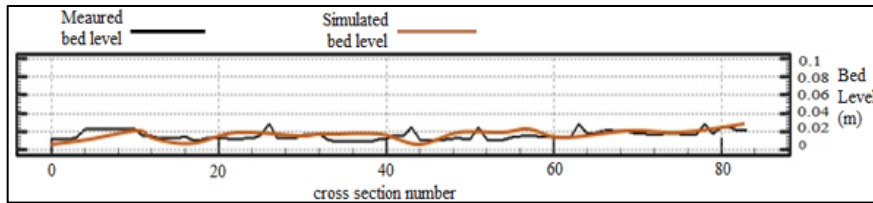


Figure 13: Simulated and observed longitudinal bed level profile at the centerline for exp. run A-1 at $t=300$ min, $n=0.029$

The Performance of the CCHE2D model has been examined with other cases. Figure 14 shows the simulated and observed morphological features of pools, point's bars, and riffles for experiment A-4 at 480 min. The simulated morphological units seem in good agreement with the experimental ones. In addition, the thalweg line of experiment A-4 at 600 min has been examined. For both experimental and numerical runs, the thalweg line changed from the right to left and then induced to right again with shallow crossings at the middle, as demonstrated in Figure 15. At the sections of pools and shoals, one side was deep (thalweg), and another side was shallow (point bar) and the variations of color regions, when compared with the layout of the experimental thalweg line, refer to an acceptable agreement.

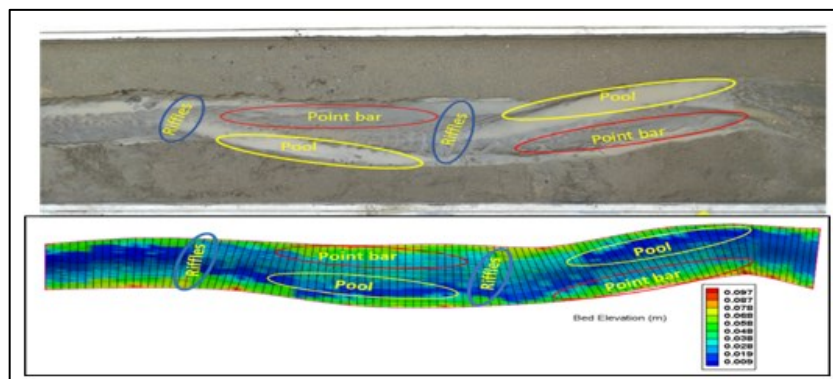


Figure 14: Simulated and observed morphological features for experiment run A-4, at 480 min

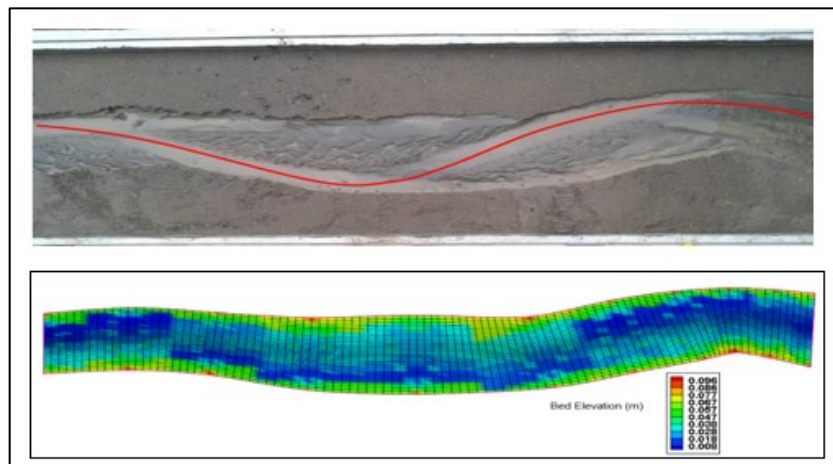


Figure 15: Simulated and observed thalweg and bank line for exp. run A-4 at equilibrium state time (600min)

4. Conclusions

CCHE2D Model has been used to investigate the hydraulic and morphological changes through meander evolution. The calibrated Manning's roughness, which gives an acceptable agreement between simulated and measured water and bed levels, was 0.029 according to the computed values of statistical indicators of BIAS, NSE, and MAE. These values were 0.0084, 0.96, and 0.0132, respectively, for water level simulation, and 0.007, 0.94, and 0.0182, respectively, for bed level simulation. The verification results were evaluated by the same statistical indicators. The obtained values of Bias, NSE, and MAE were 0.09, 0.81, and 0.018, respectively, which indicated good agreement between the simulated and measured water level profiles. In addition, the obtained values of Bias, NSE, and MAE were 0.12, 0.73, and 0.012, respectively, which indicated reasonable agreement between the simulated and measured bed level profiles. According to the computed values of BIAS, the water and bed levels are slightly tended to the overestimation. The present morphologic investigation can be used to identify dredging location in natural channels as well to decision-makers for the selection of sediment control structures and their position. In addition, finding thalweg alignment could be useful in identifying the navigation waterway. In addition to morphologic results, the water level results are as well as helpful for the water managers.

References

- [1] H. Cameron, and B. Bauer, "River bank erosion processes along the Lower Shuswap River," Final report project. university of British Colombia Okanagan, 2014
- [2] K. Blanckaert, "Hydrodynamic processes in sharp meander bends and their morphological implications," Journal of geophysical research, Vol. 116, F01003, 2011.
- [3] J. Kalkwijk, and H. Devriend, "Computation of the flow in shallow river bends," Journal of Hydraulic Resources, 18, 4, 327-341, 1980.
- [4] J. F. Friedkin, "A laboratory study of the meandering of alluvial rivers," US Army Engineer Waterways Experiment Station, Vicksburg, Mississippi, 1945.
- [5] L. Yilmaz, "Modeling of developed meanders of an alluvial channel, sediment transport, Dr. Silvia Susana Ginsberg (Ed.), ISBN: 978-953-307-189-3, available www.intechopen.com, 2011.
- [6] A. Odgaard, "River meander model. I: development," J. Hydraul. Eng., 115, 11, 1433-1450, 1989.
- [7] T. Molls, and M. H. Chaudhry, "Depth-averaged open-channel flow model," J. Hydraulic. Eng., 121, 6, 453-465, 1995
- [8] T. Y. Hsieh, and J. C. Yang, "Investigation on the suitability of two-dimensional depth-averaged models for bend-flow simulation," J. Hydraul. Eng., 129, 8, 597-612, 2003.
- [9] P. Arpan, K. K. Kishanjit, and S. Sovan, "Variation of velocity distribution in rough meandering channels," Department of Civil Engineering, Hydraulics Laboratory, National Institute of Technology Rourkela, Odisha, India, 2015.
- [10] A. Aziaian, M. Gholizadeh, and T. E. Amiri "Simulation of meandering rivers migration processes using CCHE2D," Proceedings of the 8th International River Engineering Conference, Iran, 2010.
- [11] H. Taebi, B. M. Shafae and M. Kaheh, "Simulation of flow in 90o bends using CCHE2D software," In the Proceedings of the 8th International River Engineering Conference, Iran, 2010.
- [12] C. He Li, Dong, J. Yafei, and Y. Zhang, "Modeling bed load transportation along the same-side and opposite banks of Meanders," the 36th IAHR World Congress, Hague, Netherlands, 2015.
- [13] S. A. Schumm, M. Mosley, and W. Weaver, "Experimental fluvial geomorphology," Wiley. New York, 1978.
- [14] L. C. Van Rijn, "Principles of sediment transport in rivers, estuaries and coastal seas," (ed.) Aqua Publications, Netherlands (<http://www.tooraj-sabzevari.blogfa.com>), 1993.
- [15] C. Auel, I. Albayrak, and R. M. Boes, "Turbulence Characteristics in supercritical open-channel flows: effects of froude number and aspect ratio," Journal of Hydraulic Engineering, 2013.
- [16] H. Bonakdari, L. Gislain, A. Girdhari "Developing turbulent flows in rectangular channels: a parametric study," Journal of Applied Research in Water and Wastewater 2, P 51-56., available http://arww.razi.ac.ir/article_52.html, 2014.
- [17] Y. Zhang, "CCHE-GUI graphical users interface for NCCHE model", User's Manual Technical Report No. NCCHE-TR-2008-01. The University of Mississippi, 2008.

[18] V. T. Chow, "Open channel hydraulics", McGraw-Hill Book Company, NY, 1959.